A new Taiwanese geoid model based upon airborne, satellite and terrestrial gravimetric data-sets

A. Ellmann
Department of Geodesy and Geomatics Engineering, University of New Brunswick, Fredericton, Canada
Department of Civil Engineering, Tallinn University of Technology, Ehitajate tee 5, Tallinn, Estonia

C. Hwang, Y-S. Hsiao
Department of Civil Engineering, National Chiao Tung University, 1001 Ta Hsueh Road, Hsinchu, Taiwan

Abstract. A new airborne gravity survey was conducted over Taiwan in 2004-2005. The survey results in conjunction with existing terrestrial, marine and satellite altimetry data are used for creating a consistent 2´x2´ grid of gravity anomalies referred to the Earth's surface. For this, the gravity anomalies observed at the flight level are downward continued to the topographic surface. After the gridding, to solve the boundary value problem (BVP) by Stokes's formula, the surface gravity anomalies are continued further to the sea level. The inverse of Poisson's integral formula is used at these steps. The effects of topographic masses are estimated by applying Helmert's second condensation method. A modified Stokes's formula is used for evaluating the short wavelength geoid contribution, whereas the long wavelength geoid information stems from a recent GRACE-based geopotential model. The effect (in terms of geoidal heights) of inclusion of the airborne data exceeds one metre over the mountainous part of Taiwan.

Keywords: airborne gravimetry, BVP, downward continuation, Helmert condensation, geoid modelling

1 Introduction

Over the past years several geoid models have been computed over Taiwan, see Hwang (1997) and references therein. Recent geoid computations employed the so-called '*remove-compute-restore*' (r-c-r) principles and have been carried out by the GRAVSOFT (Tscherning et al., 1992) software. According to this method the residual terrain model (RTM) gravity effect and the long wavelength gravity field from the EGM96 (Lemoine et al., 1998) model are removed from the surface-related free-air anomalies. The Fourier transform and least-squares collocation were used to transform these residual gravity anomalies into the residual geoid. After adding to it the RTM contribution and the EGM96 based reference spheroid one arrives at the quasi-geoid model, which is then converted into geoidal heights. Note that in these computations the integration is proceeded by the unmodified Stokes function and the full expansion (i.e. up to degree 360) of the EGM96 is used. The estimation of the residual topographical effects is based on the planar approximation of the topography.

This contribution aims at summarizing the application of the Stokes-Helmert approach for computing a new geoid model for Taiwan. It should be noted that the Stokes-Helmert principles deviate quite a lot from those applied in earlier studies. Due to space limitations, however, their comparison with the r-c-r scheme is considered to be outside the scope of this study. Instead, the focus here is on incorporating the airborne data into the geoid determination procedure. Second, the recent improvements of the gravity data in the global scale have significant computational implications for regional geoid modelling as well. In this context a typical computational set-up with employing up-to-date (e.g., GRACE-based) geopotential models (GGM) for regional geoid modelling is revisited.

2 Stokes-Helmert's geoid modelling principles

The solution of the BVP by Stokes's method requires gravity observations that refer to the geoid. The gravity measurements are taken at the topographic surface or even above it. Thus, to satisfy the boundary condition the gravity anomalies need to be downward continued (DWC) to the geoid level. To ensure harmonicity of the quantities to be downward continued a number of different corrections related to the existence of topography and atmosphere need to be introduced. As is well known the evaluation of the topographical effects is one of the most serious limits in precise geoid modelling nowadays.

One way of estimating the effect of topographical masses is to use Helmert's second condensation model. According to this model a condensation layer located on the geoid replaces the Earth's topographical masses. So "Helmertized" gravity field can be downward continued to the geoid level, where it will be decomposed into low- and high-frequency parts. The long wavelength geoid information comes from the adopted GGM, whereas

the short-wavelength part is obtained from the Stokesian integration over a limited domain. The truncation bias that occurs due to neglecting the remote zone is mitigated by modifying Stokes's formula. For more details on Stokes-Helmert scheme, see e.g., Vaníček and Martinec (1994), Martinec (1998), Vaníček et al. (1999) and references therein. A recent review can also be found in Ellmann and Vaníček (2006).

3 Target area and gravity data

The geographical limits of the target area are 21.5° and 25.5° northern latitudes, and 119.5° and 122.5° eastern longitudes (i.e. an area of 440 x 300 km^2), see Fig. 1. The new geoid model comprises the whole of Taiwan together with a large portion of surrounding waters. Taiwan's terrain is complex and mostly inaccessible for conventional gravity survey.

Over 75% of Taiwan's terrain is covered with hills and high mountains, with the highest point being nearly 4000 m. Here the existing gravity data are sparsely distributed and there have been uncertainties in the gravity datum and the coordinate system associated with point gravity data (Hwang et al., in press). Obviously, the shortages of the data in the (mountainous) centre of the target area affect negatively the reliability of the overall geoid determination results.

In order to enhance the spatial resolution of gravity data both on land and sea, an airborne gravity survey campaign was carried out in 2004-2005 over Taiwan using a LaCoste & Romberg air-sea gravimeter. The average flight altitude was 5156 m (± few tens of meters, due to in-flight turbulence), the survey area (~75,000 km^2) covers the major part of the target area (for an illustration see e.g., Hwang et al., in press, Fig. 1). The overall airborne gravity accuracy is estimated to be 2 mGal at a spatial (half wavelength) resolution of 6 km. A more detailed report of the survey particulars and quality assurance can be found in Hwang et al. (in press).

Fig. 1. Distribution of the terrestrial and marine gravity data-points in the target area (enclosed by the rectangle). The white polyhedral bounds the mountainous area (average H > 1200 m), where the airborne data will be used for the gridding.

Recall, that the main objective of this study is to investigate the geoid improvements due to inclusion of the new airborne gravity data. For the sake of comparison two new geoid models are computed. The first model will be based on the existing terrestrial, marine and satellite altimetry gravity data, hence to be referred to as *NoAirborne* geoid model. The second model combines exactly the same data-sets plus airborne gravity data. This model is referred to as *Airborne* geoid model.

The computational scheme of the *Airborne* geoid model is as follows: (i) DWC the airborne data to the earth's surface; (ii) construct the existing and airborne data into a uniform grid at the earth's surface; (iii) DWC the anomaly grid to the geoid level; (iv) Stokesian integration on the geoid level. The computational scheme for the *NoAirborne* model begins from step (ii). Since both models employ the Stokes-Helmert principles, their discrepancies indicate the geoid improvements due to the inclusion of the new airborne gravity data.

4 Downward continuation of Helmert's anomaly

4.1 Helmert's anomaly

Application of the Helmert reduction yields a new gravity field, which becomes slightly different from the actual gravity field. As a result, the corresponding Helmert anomalies, $\Delta g^h(r,\Omega)$, differ from the commonly used free-air anomalies, $\Delta g(r,\Omega)$. The relation between the two anomaly types can be expressed as (cf. Vaníček et al., 1999):

$$\Delta g^h\left(r_f,\Omega\right)=\Delta g\left(r_f,\Omega\right)+\frac{\partial\left[V^t\left(r_f,\Omega\right)-V^{ct}\left(r_f,\Omega\right)\right]}{\partial r}+\frac{2}{r_f\left(\Omega\right)}\left[V^t\left(r_f,\Omega\right)-V^{ct}\left(r_f,\Omega\right)\right]+e_{ellips}\left(r_f,\Omega\right), \quad (1)$$

where $V^t(r,\Omega)$ and $V^{ct}(r,\Omega)$ are the potentials of topographic masses and condensation layer,

respectively. The geocentric position (r,Ω) is represented by the geocentric radius $r(\Omega)$ and a pair of geocentric coordinates $\Omega = (\varphi,\lambda)$, where φ and λ are the geocentric spherical coordinates. All the quantities in Eq. (1) are referred to the flight level, $r_f(\Omega)=r_g(\Omega)+5156$ m, where $r_g(\Omega)$ is the geocentric radius of the geoid surface. The term $\varepsilon_{ellips}(r_f,\Omega)$ represents the ellipsoidal correction, which accounts for the deviation of the actual shape of the Earth from the spherical approximation of the fundamental gravimetric equation (for more details, see Vaníček et al., 1999). The formulation of the topographic terms in Eq. (1) employs the spherical approximation (Martinec, 1998). They can be evaluated by using the topographic elevation/density models in some numerical quadrature method (see e.g., Martinec, 1998). More specifically, the integration domain is usually divided among different element sizes, with small as possible elements close to the computation point. The topographic effects are estimated by using a new 3"x3" Taiwanese digital elevation model, it serves also as a basis for generating the sets of 30"x30" and 2´x2´ mean heights, which are used for more distant masses with respect to the computation points.

Note that the atmospheric effects are neglected in Eq. (1). This is due to the fact that the IAG atmospheric correction (Moritz, 1992) is already considered in the Taiwanese gravity data.

The gravity field over Taiwan is fairly complicated due to various regional geophysical phenomena. Recall also that the free-air anomalies are strongly correlated with the topography. Therefore, even at the flight altitude, the free-air anomalies are rather powerful, ranging from 257 to –173 mGal. It should be noted, however, that the corresponding Helmert anomaly field (obtained by Eq. (1)) is somewhat smoother than the initial free-air anomalies.

4.2 Downward continuation

Recall that step (ii) aims at combining the downward continued data points with the existing terrestrial data-points to form a uniform data grid at the earth's surface. In this study the downward continuation is solved by using the Poisson equation (Heiskanen and Moritz, 1967, p. 317). This integral formula had been originally designed as a formula for the upward continuation of harmonic quantities. In practice the integration is replaced by a summation over a regularly spaced grid of geographical coordinates. The resolution of the air-borne survey allows forming a 2´x2´ anomaly grid, which thereafter will be used for downward continuation.

Importantly, the gridding helps to overcome the following shortage. Namely, the Poisson downward continuation is known to be an unstable problem. Due to the instability, existing errors in $\Delta g^h(r_f,\Omega)$, may appear magnified in the solution. However, when mean values (obtained from gridding) are used instead of point values, this problem is somewhat alleviated, as the mean values do not exhibit the highest frequencies (Sun and Vaníček, 1998). For solving Poisson's formula it is expressed as a system of linear equations (cf. Martinec, 1996):

$$\Delta \mathbf{g}^h\left(r_f,\Omega\right)=\mathbf{K}\left[r_f,y\ (\Omega,\Omega'),r_i\right]\ \Delta \mathbf{g}^h\left(r_i,\Omega'\right)\ , \quad (2)$$

where $\Delta \boldsymbol{g}^h(r_f,\Omega')$ is the vector of Helmert's anomaly at the flight altitude (5156 m), $\Delta \boldsymbol{g}^h(r_i,\Omega')$, is the vector of the gravity anomalies referred to an i-th layer with a geocentric radius r_i, $\mathbf{K}\left[r_f,y\ (\Omega,\Omega'),r_i\right]$ is the matrix of the values of the Poisson integral kernel multiplied by the area of integration element, $\psi(\Omega,\Omega')$ is the geocentric angle between the computation and integration points. Downward continuation is an inverse problem to the original Poisson integral. The matrix-vector form of Poisson's equation can then be used for solving the inverse problem, i.e. computing the unknown elements of the vector $\Delta \boldsymbol{g}^h(r_i,\Omega)$.

Recall that the application of the Helmert condensation suppresses (mathematically) the topographical masses into the geoid. Therefore the product of the Helmert anomaly and geocentric radius, $\Delta g^h \cdot r$, is harmonic (Vaníček et al., 1996) and such a field can be downward continued (conversely, this is not the case for the free-air anomaly!) to any elevation within the interval of $r_g < r_g+H < r_f$.

Anomaly values at the earth's surface are obtained as follows. Layer-wise DWC will be used to form a number of horizontal (2D) anomaly grids at different altitudes r_i, cf. Eq. (2). The separation between the adjacent layers (which are also parallel to the geoid) is set to 200 m. Since the mean 2'x2' heights over Taiwan do not exceed 3400 m then the uppermost grid of downward continued gravity anomalies is formed at H = 3400 m. The next grid of gravity anomalies is formed at 3200 m. Further on, similar 2D grids are formed at the altitudes 3000 m, 2800 m, etc. all the way down to 1200 m (this limit is chosen empirically, see below). Remember, for each layer the Helmert anomalies at the flight level serve as initial values. In other words a 3D structure, a mesh, consisting of 14 horizontal layers is formed. The anomaly values at topographic surface points ($1200 < H < 3400$ m) are predicted by a simple "sandwich"-grid 3D interpolation. The resulting Helmert anomalies are referred to the surface of the Earth, $r_t(\Omega) = r_g(\Omega) + H(\Omega)$. 173 terrestrial points (located above 1200 m) were used for evaluating the accuracy of the downward continued anomalies. The differences between the estimated and "true" values

approach ± 30 mGal, their statistical mean and the RMS error are 0.9 and 9.8 mGal, respectively. Since the gravity variations are rather large (for an illustration, see Hwang et al., in press, Fig.3) within this particular area, then most likely, a part of the detected discrepancies stem from the discretization as well. Recall, that the terrestrial data is of good quality and sufficiently dense in lowland (coastal) regions. However, to compensate the lack of the gravity data over the mountains, the downward continued data will be used in the regions above 1200 m.

It should be noted that other strategies of combining different data-sets are still being tested and the results will be reported on in proper time. For instance, an alternative scheme is considered: (i) separate DWC of the airborne and terrestrial data-points to the geoid level; (ii) forming a uniform grid of gravity anomalies at the geoid level; (iii) using this grid for solving the BVP.

5 Gridding of anomalies

Many numerical procedures at geoid modelling require gravity/topographic data on regularly spaced grid of geographical coordinates. Within the target area the total number of the terrestrial, marine and satellite altimetry (KMS02, see Anderson and Knudsen, 1998) gravity points exceeds 10000. The average number of gravity points per one degree square is about 1000 (1 point per 10 km^2), which suggests that a 2´x2´ grid resolution is a reasonable choice. The gridding is proceeded by a National Chiao Tung University collocation program, whereas different weights are assigned for different data types.

Gridding is a critical issue, because any error committed at this stage will directly propagate into the geoid solution. Within the frame of an experiment, not described here, the gridding for the *NoAirborne* model was proceeded with the free-air anomalies. Better interpolation results, however, are usually achieved by using the smoother Bouguer anomalies. Therefore the *Airborne* model utilises the complete spherical Bouguer anomalies (Vaníček et al., 2004) for gridding. This anomaly is also called as *NoTopography* (NT) anomaly, since the attraction of the global topography has been completely subtracted from the "full" gravity. A more detailed discussion on the used gridding approach is spared for a forthcoming paper. The resulting grids of the NT-anomalies (*Airborne* scheme) and free-air anomalies (*NoAirborne* scheme) are converted into surface-related Helmert anomalies, see Eq. (1). $\Delta g^h(r_t,\Omega)$ are thereafter downward continued to the geoid level. The same approach is used as described in Section 4.2, whereas the symbols r_f and r_i in Eq. (2) need to be replaced by r_t and r_g, respectively.

6 Solution to Stokes's boundary value problem

The Helmert gravity anomalies on the geoid level serve as an input when solving the Stokes boundary value problem. Strictly speaking, the original Stokes formula requires gravity anomalies over the entire Earth (Ω_0). In practice, however, the area of availability of anomalies is limited to some spatial domain ($\Omega_{\psi 0}$) around the computation point. The truncation bias (that occurs when the remote zone, Ω_0 - $\Omega_{\psi 0}$, is neglected in the integration) can be reduced by modifying Stokes's formula (Molodensky et al., 1960). This study employs the generalized Stokes scheme (cf. Vaníček and Sjöberg, 1991), which uses the long wavelength part of a GGM as follows:

$$N(\Omega)=\frac{V^t(r_g,\Omega)-V^{ct}(r_g,\Omega)}{g_0(f)}+\frac{R}{2g_0(f)}\sum_{n=2}^{M}\frac{2}{n-1}\Delta g_n^h + \frac{R}{4\pi g_0(f)}\iint_{\Omega_{y_0}} S^M(y_0,y\ (\Omega,\Omega'))\left(\Delta g^h-\sum_{n=2}^{M}\Delta g_n^h\right)d\Omega' \quad ,(3)$$

where R is the mean radius of the Earth; the modified Stokes function $S^M(y_0,y,(\Omega,\Omega'))$, can be computed according to Vaníček and Kleusberg (1987); $g_0(f)$ is the normal gravity (a function of latitude) at the reference ellipsoid, $d\Omega'$ is the area of the integration element. Note also that the used geopotential coefficients need first to be Helmertised to compute the harmonics $\Delta g_n^h(r_g,\Omega)$. For more details see Vaníček et al. (1995).

The Stokesian integration with Helmert's residual anomalies (i.e. the last term on the right hand side of Eq. (3)) results in the Helmert residual co-geoid. Since the low-degree reference gravity field is removed from the anomalies before the Stokes integration, then the long-wavelength geoid information, i.e. the reference spheroid of degree M (see Heiskanen and Moritz, 1967, p. 97), is added to the residual geoid.

As already noted, the condensation of the topographic masses causes the Helmert potential to become slightly different from the actual potential. Consequently, also the Helmert co-geoid does not exactly coincide with the real geoid. The effect causing this change is called primary indirect topographic effect. Thus, the first term in the right hand side of Eq. (3) transfers the Helmert co-geoid into the actual geoidal heights.

The selection of the upper limit, M, which is used for defining the reference spheroid/anomaly and the modified Stokes function, $S^M(y_0,y,(\Omega,\Omega'))$, is

important in geoid modelling. The following criteria were considered at the selection of the suitable limit (M) and corresponding integration radius ψ_0. Obviously, the regional geoid models are also dependent, among other factors, on the quality of the used GGM. Recall that the high-degree GGM-s are determined from a combination of satellite data and terrestrial gravity data. This combination implies that the reference GGM and $Dg^h(r,\Omega)$ in Eq. (3) could be correlated with each other. One may want to avoid this undesirable feature. Therefore it is recommendable to use the "satellite-only" harmonics for computing the reference quantities in Eq. (3).

A new combination model EIGEN-CG03C (Förste et al., 2005) is based on the CHAMP mission and the global surface data, but takes also into account 376 days of the GRACE twin-satellites tracking data. The EIGEN-CG03C spherical harmonics are developed up to degree/order 360/360, which corresponds to a spatial resolution of 110 km. The EIGEN-CG03C "satellite-only" field is developed up to degree/order 150/150. However, the user of a GGM should not consider the "satellite-only" harmonics as an errorless dataset, especially at the higher degrees. Therefore one cannot increase the modification limit in Eq. (3) all the way up to maximum available spherical harmonic degree. For instance, the EIGEN-CG03C developers estimate an 1 cm accuracy in geoid modelling with a spectral resolution up to degree/order 75/75. For more details see the original publication.

Various aspects need to be considered when selecting the integration radius. Generally, a compromise is needed to balance between the shortages of the low- and high-degree parts of the gravity data. Fig. 1 demonstrates that the limited extension (especially to the west from the target area) of the gravity data is the most serious constraint for the present study.

The choice of y_0 = 1.5° is the basis for determining the upper modification limit M. According to an approach in Featherstone et al. (1998) we want the modified Stokes function $S^M(y_0,y,(\Omega,\Omega'))$ to become zero at the edge of the integration cap. The kernel is enforced to zero at y_0 = 1.5° with M = 90. This is satisfactory to us, since at the degree 90 the correlation between the EIGEN-CG03C-derived and terrestrial datasets is completely prevented. Even though this limit exceeds somewhat the sub-cm accuracy expectation, it is tolerable due to limited availability of the regional gravity data. To eliminate the edge effect the gravity anomalies outside of the target area (where available) were also included into Stokes's integration.

It should be noted, however, that in the case of sufficient data coverage a larger integration radius in conjunction with a smaller modification limit could provide more reliable results.

7 Discrepancies between the *Airborne* and *NoAirborne* geoid models

The resulting discrepancies between the *Airborne* and *NoAirborne* geoid models range between –1.1 and +2.3 m, see Fig. 2. Naturally, the largest discrepancies occur over the mountains, more specifically, inside the loops of the terrestrial gravity survey. Obviously, the new airborne gravity data have affected significantly the results over the mountainous regions, where only a few terrestrial points are available. Note also that at the closest vicinity of the terrestrial survey loops the discrepancies remain relatively small. This indicates that there is a reasonable agreement between the downward continued and the terrestrial anomaly values. Nevertheless, the possible errors of the downward continuation may also contribute to the detected discrepancies.

Recall that different types of gravity anomalies were used for gridding of the *Airborne* and *NoAirborne* models as well. Therefore, the discrepancies between the *NoAirborne* and *Airborne* geoid models are not only due to inclusion of the airborne data, but also due to adoption of different anomaly types for gridding. This is in agreement with a recent study by Janák and Vaníček (2005), who demonstrate that different gridding strategies may have a significant effect (up to 1-2 metres) on the geoidal heights.

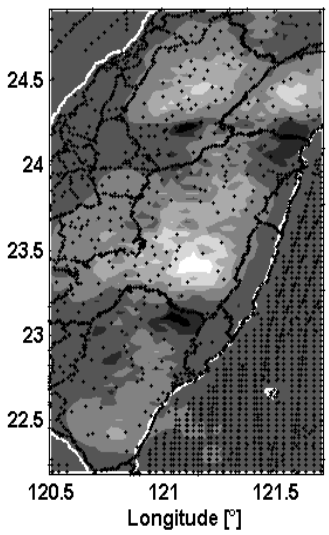

Fig. 2. Discrepancies between the two geoid models ("*NoAirborne*" minus "*Airborne*") over the central part of Taiwan. The discrepancies range from -1.1 m (the darkest region) to +2.3 m (the brightest region). Black dots denote the locations of the point gravity data (downward continued airborne gravity points are not shown).

8 Summary and further studies

This contribution discusses the effect of inclusion of the airborne data on anomaly gridding over the mountainous parts of Taiwan, and the corresponding effects on geoid heights. Stokes-Helmert's geoid determination principles were applied for computing two new geoid models over Taiwan. The emphasis was given to the downward continuation of the harmonic Helmert anomaly and solving Stokes's BVP by using up-to-date GRACE-based reference models. We conclude, that the downward continued airborne gravity data in conjunction with surrounding terrestrial measurements are useful for geoid improvements over the areas with insufficient coverage of terrestrial data.

Evidently, the region of interest, due to its very complicated geophysical conditions, appears to be very challenging in the context of the geoid modelling. Geoid modelling in Taiwan is a continuous effort and the goal is to achieve a cm-level accuracy everywhere in Taiwan. Hence, the results here are only a part of the on-going work. Future studies include: (i) validation of the geoid models by using high-precision GPS-levelling data; (ii) comparisons with earlier geoid models in order to detected the most suitable geoid approach (e.g., r-c-r vs. Stokes-Helmert) (iii) usage of different reference models (e.g., EGM96 vs. GRACE-based models) and modification limits; (iv) application of different gridding approaches. Furthermore, another airborne gravity survey campaign (at the flight altitude ~1500 m) was carried out over the Kuroshio Current east of Taiwan in 2006. It is of interest to utilise the new results in the Taiwanese geoid determination as well. The results of the aforementioned studies will be reported in forthcoming papers.

Acknowledgements This study is funded by the Ministry of Interior, Taiwan, under the project "Airborne gravity survey in Taiwan". The prime author is supported by the European Union Structural Funds, Project # 1.0101-0335. Thoughtful comments by Dr. D. Roman and an anonymous reviewer are gratefully thanked.

References

Andersen OB, Knudsen P (1998) Global Marine Gravity Field from the ERS-1 and GEOSAT Geodetic Mission Altimetry, *Journal of Geophysical Research*, **103(C4)**, 8129-8137.

Ellmann A, Vaníček P (2006) UNB application of Stokes-Helmert's approach to geoid computation. *Journal of Geodynamics*, DOI:10.1016/j.jog.2006.09.019.

Featherstone WF, Evans JD, Olliver JG (1998) A Meissl modified Vaníček and Kleusberg kernel to reduce the truncation error in gravimetric geoid determination. *Journal of Geodesy*, **72**, 154-160.

Förste C, Flechtner F, Schmidt R, Meyer U, Stubenvoll R, Barthelmes F, König R, Neumayer KH, Rothacher M, Reigber C, Biancale R, Bruinsma S, Lemoine JM, Raimondo JC (2005) *A New High Resolution Global Gravity Field Model Derived From Combination of GRACE and CHAMP Mission and Altimetry/Gravimetry Surface Gravity Data*. A Poster presented at EGU General Assembly 2005, Vienna, Austria, 24-29, April.

Heiskanen WH, Moritz H (1967) *Physical geodesy*. Freeman and Co, San Francisco.

Hwang C (1997) Analysis of some systematic errors affecting altimeter-derived sea surface gradient with application to geoid determination over Taiwan. *Journal of Geodesy*, **71**, 113-130.

Hwang C, Hsiao Y-S, Shih H-C, Yang M, Chen K-H, Forsberg R, Olesen AV (in press): Geodetic and geophysical results from a Taiwan airborne gravity survey: Data reduction and accuracy assessment. Accepted by: *Journal of Geophysical Research - Solid Earth*.

Janák J, Vaníček P (2005) Mean free-air gravity anomalies in the mountains. *Studia Geophysica et Geodaetica*, **49**, 31-42.

Lemoine FG, Kenyon SC, Factor JK, Trimmer RG, Pavlis NK, Chinn DS, Cox CM, Klosko SM, Luthcke SB, Torrence MH, Wang YM, Williamson RG, Pavlis EC, Rapp RH, Olson TR (1998) *The Development of Joint NASA GSFC and the National Imagery and Mapping Agency (NIMA) Geopotential Model EGM96*. NASA/TP-1998-206861, Greenbelt, MD.

Martinec Z (1996) Stability investigations of a discrete downward continuation problem for geoid determination in the Canadian Rocky Mountains. *Journal of Geodesy*, **70**, 805-828.

Martinec Z (1998) *Boundary value problems for gravimetric determination of a precise geoid*. Lecture notes in Earth sciences, Vol. 73, Springer, Berlin, Heidelberg, New York.

Molodensky MS, Yeremeev VF, Yurkina MI (1960) *Methods for Study of the External Gravitational Field and Figure of the Earth*. TRUDY TsNIIGAiK, 131, Geodezizdat, Moscow. English translat.: Israel Program for Scientific Translation, Jerusalem 1962.

Moritz H (1992) Geodetic Reference System 1980. *Bulletin Géodésique*, **66**, 187-192.

Sun W, Vaníček P (1998) On some problems of the downward continuation of the 5'x 5' mean Helmert gravity disturbance. *Journal of Geodesy*, **72**, 411-420.

Tscherning CC, Forsberg R, Knudsen P (1992) The GRAVSOFT package for geoid determination. *Proceedings of the First Continental Workshop on the Geoid in Europe*, Prague, pp. 327-334, Springer-Verlag, New York.

Vaníček P, Kleusberg A (1987) The Canadian geoid – Stokesian approach. Compilation of a precise regional geoid. *Manuscripta Geodaetica*, **12**, 86-98.

Vaníček P, Sjöberg LE (1991) Reformulation of Stokes's Theory for Higher Than Second-Degree Reference Field and Modification of Integration Kernels. *Journal of Geophysical Research*, **96(B4)**, 6529-6339.

Vaníček P, Martinec Z (1994) The Stokes-Helmert scheme for the evaluation of a precise geoid. *Manuscripta Geodaetica*, **19**, 119-128.

Vaníček P, Najafi M, Martinec Z, Harrie L, Sjöberg LE (1995) Higher-degree reference field in the generalised Stokes-Helmert scheme for geoid computation. *Journal of Geodesy*, **70**, 176-182.

Vaníček P, Sun W, Ong P, Martinec Z, Najafi M, Vajda P, Horst B (1996) Downward continuation of Helmert's gravity. *Journal of Geodesy*, **71**, 21-34.

Vaníček P, Huang J, Novák P, Pagiatakis SD, Véronneau M, Martinec Z, Featherstone WE (1999) Determination of the boundary values for the Stokes-Helmert problem. *Journal of Geodesy*, **73**, 160-192.

Vaníček P, Tenzer R, Sjöberg LE, Martinec Z, Featherstone WE (2004) New views of the spherical Bouguer gravity anomaly, *Geophysical Journal International*, **159**, 460-472.